Synthesis, Anticancer and Antibacterial Activity of Some Novel Mononuclear Ru(II) Complexes

Upal Kanti MAZUMDER,[a] Malaya GUPTA,*[,b] Subhas Somalingappa KARKI,[a] Shiladitya BHATTACHARYA,[a] Suresh RATHINASAMY,[a] and Sivakumar THANGAVEL[b]

[a] *Division of Pharmaceutical Chemistry, and* [b] *Division of Pharmacology, Department of Pharmaceutical Technology, Jadavpur University; Jadavpur, Kolkata–700 032, India.* Received July 4, 2003; accepted November 5, 2003

In search of potential anticancer drug candidates in ruthenium complexes, a series of mononuclear ruthenium complexes of the type $[Ru(phen)_2(nmit)]Cl_2$ (Ru1), $[Ru(bpy)_2(nmit)]Cl_2$ (Ru2), $[Ru(phen)_2(icpl)]Cl_2$ (Ru3), $Ru(bpy)_2(icpl)]Cl_2$ (Ru4) (phen=1,10-phenanthroline; bpy=2,2′-bipyridine; nmit=*N*-methyl-isatin-3-thiosemicarbazone, icpl=isatin-3-(4-Cl-phenyl)thiosemicarbazone) and $[Ru(phen)_2(aze)]Cl_2$ (Ru5), $[Ru(bpy)_2(aze)]Cl_2$ (Ru6) (aze=acetazolamide) and $[Ru(phen)_2(R\text{-}tsc)](ClO_4)_2$ (R=methyl (Ru7), ethyl (Ru8), cyclohexyl (Ru9), 4-Cl-phenyl (10), 4-Br-phenyl (Ru11), and 4-EtO-phenyl (Ru12), tsc=thiosemicarbazone) were prepared and characterized by elemental analysis, FTIR, ^{1}H-NMR and FAB-MS. Effect of these complexes on the growth of a transplantable murine tumor cell line (Ehrlich Ascites Carcinoma) and their antibacterial activity were studied. In cancer study the effect of hematological profile of the tumor hosts have also been studied. In the cancer study, the complexes Ru1—Ru4, Ru10 and Ru11 have remarkably decreased the tumor volume and viable ascitic cell count as indicated by trypan blue dye exclusion test ($p<0.05$). Treatment with the ruthenium complexes prolonged the lifespan of Ehrlich Ascites Carcinoma (EAC) bearing mice. Tumor inhibition by the ruthenium chelates was followed by improvements in hemoglobin, RBC and WBC values. All the complexes showed antibacterial activity, except Ru5 and Ru6. Thus, the results suggest that these ruthenium complexes have significant antitumor property and antibacterial activity. The results also reflect that the drug does not adversely affect the hematological profiles as compared to that of cisplatin on the host.

Key words ruthenium complex; hematological profile; anticancer activity

The success of cisplatin and related platinum complexes as anticancer agents has stimulated a search for other active transition metal complexes, and ruthenium in particular has attracted the researchers.[1)] Metal complexes of ruthenium containing nitrogen and oxygen donor ligands are found to be effective catalysts for oxidation, reduction, hydrolysis and other organic transformation.[2)] The coordination environment around ruthenium plays the key role in stabilizing its different oxidation states and hence dictates the redox properties of the control atoms.[3,4)] Since then, complexes such as *trans*-(IndH)$[Ru(ind)_2Cl_4]$ (Ind=indazole), mer-$[Ru(terpy)]Cl_3$ (terpy=2,2′-terpyridine), and $Ru(chdH_2)Cl_2$ (chd=1,2-cyclohexanediamine tetraacetate), have been reported to be highly active.[5—7)] Other classic ruthenium complexes such as $Ru(dmso)_4Cl_2$[8)] (dmso=dimethylsulfoxide), $ImH[Ru(im)Cl_5]$,[9)] $ImH[Ru(im)_2Cl_4]$[10)] and $ImH[Ru(im)(dmso)Cl_4]$[11)] (NAMI-A) (im=imidazole) are also well known antitumor agents. Complexes like $[Ru(arene)(l)]Cl_2$[12)] (arene=*p*-cymene, hexamethylbenzene and l=carbene or nitrogen containing heterocycles) have been tested for antibacterial and antifungal activity.

The tris chelates of the ruthenium with bidentate ligands show intercalate properties with the DNA[13)] and bind to Fe(III) sites of the proteins lactoferin and transferrin[14,15)] and transferrin is thought to be responsible for the delivery of Ru(III) to cancer cells where it is taken up *via* receptor mediated endocytosis.[16)] Transferrin normally transports Fe(III) in the blood but is only about one third occupied by Fe(III), and so there are vacant sites available for Ru(III) binding. Another important step in the mechanism of action of Ru(III) complexes is thought to be *in vivo* reduction to Ru(II),[17)] which is kinetically more reactive than Ru(III). Recently we have reported, *N*-alkyl and *N*-aryl substituted thiosemicarbazide complexes with $Ru(bpy)_2Cl_2$ and greater antibacterial activity was found in the *N*-alkyl substituted complexes whereas *N*-aryl substituted exhibited more antitumor activity.[18)] In view of the above facts we have investigated the design of a novel range of Ru(II) complexes and the structural features as well as the contribution of the ligands that are responsible for antitumor and antibacterial activity.

Results and Discussion

Chemistry The ligands nmit (nmit=*N*-methyl-isatin-3-thiosemicarbazone) and icpl (icpl=isatin-3-(4-chlorophenyl) thiosemicarbazone) were prepared by reacting *N*-methylisatin and isatin with thiosemicarbazide and 4-chlorophenyl thiosemicarbazide in alcohol in presence of glacial acetic acid in 1 : 1 molar ratios respectively. Other ligands like r-tsc (r-tsc=4-substituted thiosemicarbazides) were prepared according to the literature[19,20)] with slight modification (Chart 1). All these ligands were confirmed for their purity by their melting point, elemental analysis and infrared spectra.

Ruthenium metal complexes with the ligands nmit, icpl, aze (aze=acetazolamide) and r-tsc were prepared by the reaction of a stoichiometric quantity of $Ru(phen)_2Cl_2$/$Ru(bpy)_2Cl_2$ with the respective ligands in alcohol in presence of nitrogen (Chart 2). The completion of the reaction was monitored by TLC on silica gel.

The structures of these ligands, especially nmit, icpl and r-tsc in Fig. 1, show that in no case these ligands can exhibit tridentate behavior. There are very few cases in which the thiosemicarbazides act as monodentate ligands binding to the metal centre through the sulfur atom, the only known solid complexes of thiosemicarbazides coordinating through the sulfur atom only are the polymeric Ag(I) complex.[21,22)] They are capable of exhibiting bidentate behavior, as shown in Fig. 2. In case of r-tsc the chelating mode is *via* sulfur atom and

* To whom correspondence should be addressed. e-mail: subhasskarki@hotmail.com

terminal hydrazinic nitrogen atom of thiosemicarbazide chain, in nmit and icpl, the chelating mode is *via* sulfur atom and imine nitrogen.[23)]

The infrared spectra of all the ligands and their ruthenium(II) complexes were recorded in KBr and reported in their respective titles by tentative assignments. Nmit and icpl ligands having vibrational frequency from 3400—3151 cm^{-1} is assigned for NH and NH_2 of thioamide stretching and at

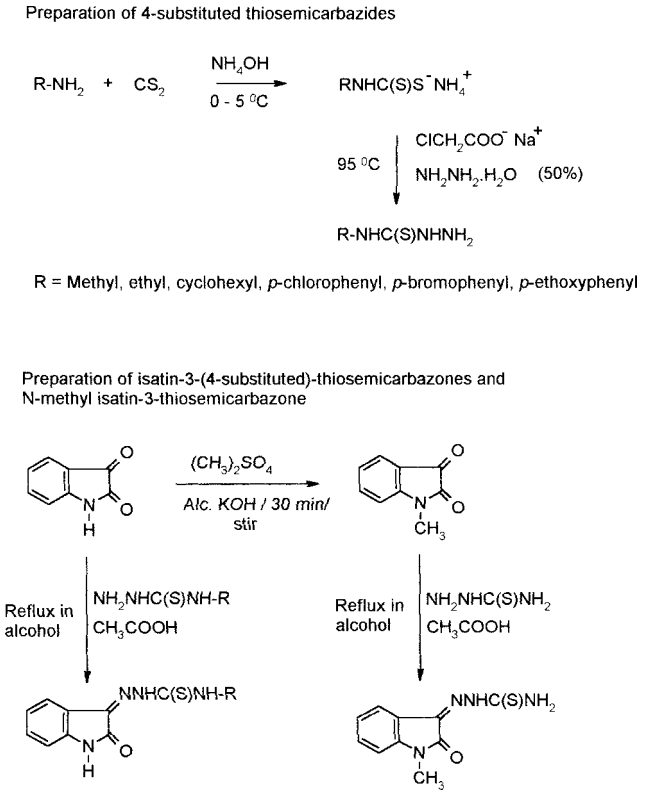

Chart 1

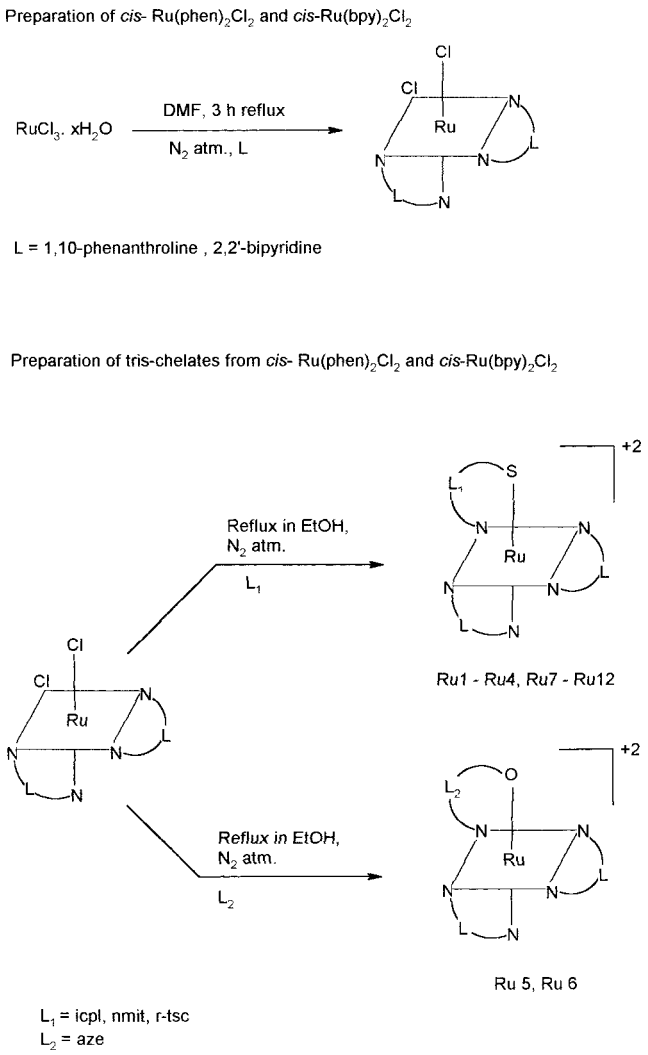

Chart 2

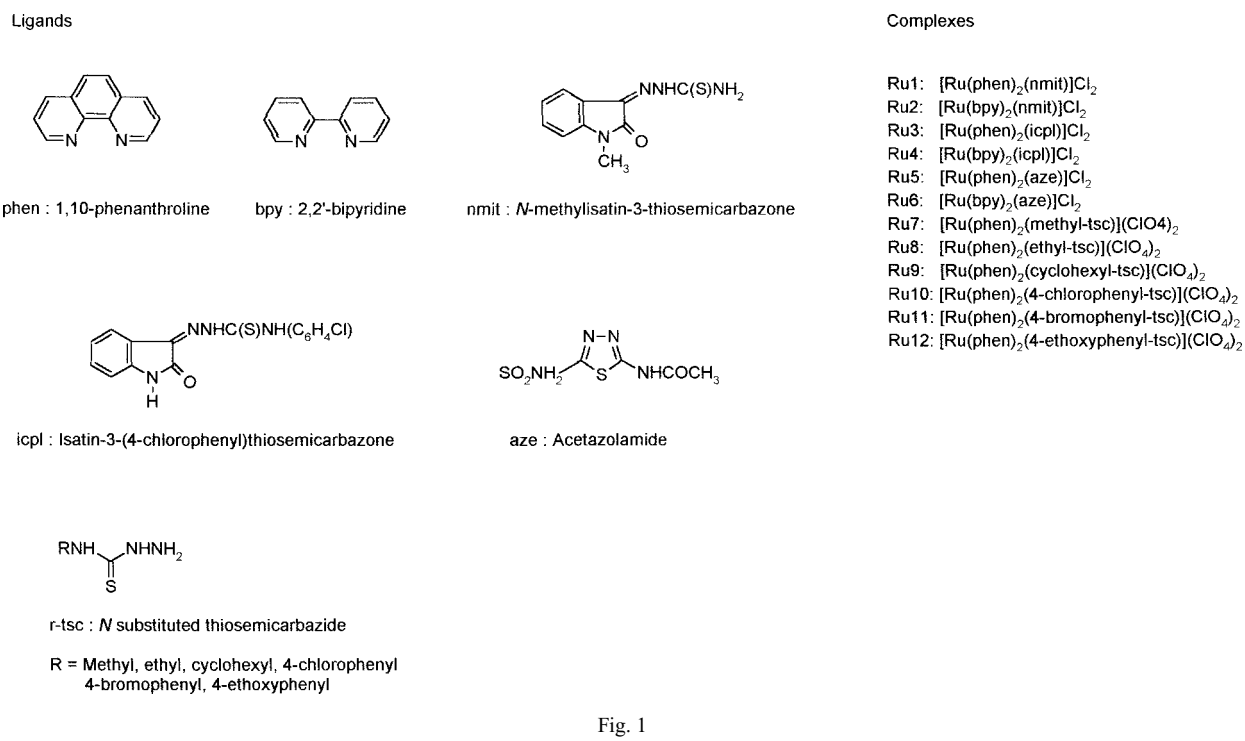

Fig. 1

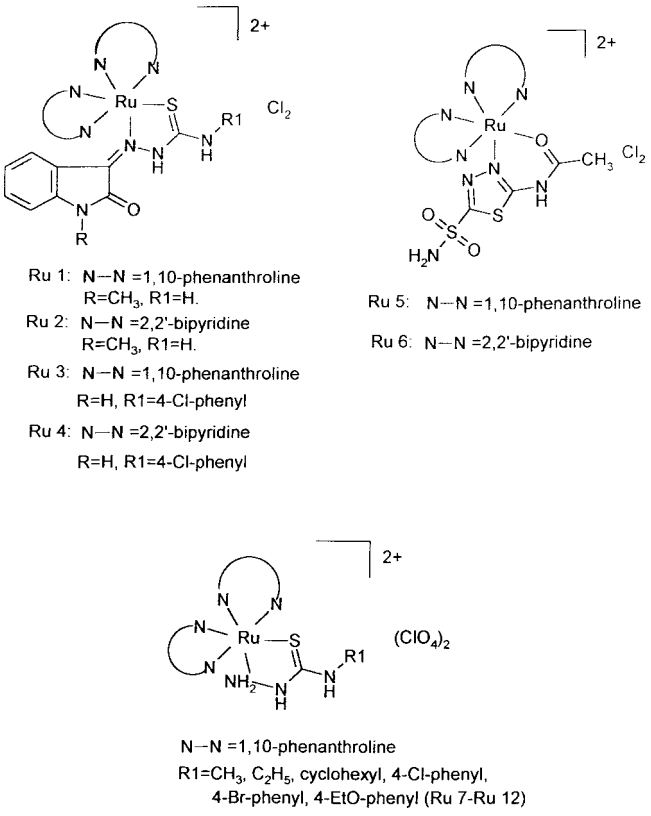

Fig. 2

the regions of 1677—1679 cm^{-1} for amide carbonyl group respectively. The IR spectra of the ligand aze have 3310—3100 cm^{-1} for NH_2 stretching, and at 1679 cm^{-1} for C=O stretching. A comparison of the IR spectra of the ligands nmit and icpl with ruthenium(II) complexes indicates, these ligands are coordinated to the metal ion by sulfur and imine nitrogen but not with amide carbonyl oxygen, which was confirmed by the IR spectra which indicates no change in vibrational frequency of amide carbonyl group.

In the complexes such as Ru5 and Ru6, the coordination has occurred *via* ring nitrogen and carbonyl oxygen but not with sulfonamide group, which was confirmed by the change in vibrational frequency of carbonyl group and not with sulfonamide. It is well known that 4-substituted-thiosemicarbazides ligands in the free state exist in the *trans*-configuration with respect to the thiocarbonyl sulfur and the terminal nitrogen atom of the thiosemicarbazide moiety. But during complex formation they became *cis* to each other.[24] In the IR spectra of the ligands r-tsc there are two strong bands in the 3000—3300 cm^{-1} region, which corresponds to $-NH_2$ stretching vibrations, besides one or two NH vibration bands in the same region. A strong band near 1600—1640 cm^{-1} corresponds to $-NH_2$ bending vibration and a band at 1370—1400 cm^{-1} corresponds to C=S stretching vibration.[25] On complexation both the $-NH_2$ bending and C=S stretching vibrations were changed. These observations clearly indicate the participation of the NH_2 group and thiocarbonyl sulfur in coordination to the metal ion.

Coordination of ligands (L=nmit, icpl and aze) to ruthenium results in complexes such as *cis*-$[Ru(phen)_2(L)]Cl_2$/*cis*-$[Ru(bpy)_2(L)]Cl_2$ (Ru1—Ru4, Ru5 and Ru6) respectively. Coordination of r-tsc ligand to *cis*-$Ru(phen)_2Cl_2$ leads to *cis*-$[Ru(phen)_2(r\text{-}tsc)]ClO_4$ (Ru7—Ru12) respectively. All these complexes do not possess any C_2 axes of symmetry. Such a loss of C_2 axis of symmetry was seen for $[Ru(bpy)_2(atatp)](ClO_4)_2$[26] (bpy=2,2′-bipyridine, atatp=acenaphtheno[1,2-b]-1,4,8,9-tetraazatriphenylene), $[Ru(L)_2(9\text{-}CH_3\text{-adenine})]^{2+}(ClO_4)_2$ (L=2,2′-bipyridine/azapyridine)[27] which leads to nonequivalency of the ligands. The complexes bearing aze and r-tsc ligands have not shown NH_2 and NH protons in their proton NMR spectra. These may have been merged with the baseline. For the complexes Ru5 and Ru6 each have 10 well resolved resonance peaks, which correspond to four different aromatic ring protons of the two 1,10-phenanthroline ligands and one resonance peak for CH_3 of acetazolamide respectively.

These complexes show broad and intense visible bands between 350 to 500 nm due to metal to ligand charge transfer transition. In the UV region the bands at 290 nm and 310 nm are assigned to 2,2′-bipyridine/1,10-phenanthroline ligand π–π^* charge transfer transitions. The same transition is found in free 2,2′-bipyridine/1,10-phenanthroline at 280 nm, so that coordination of the ligand results in a red shift in the transition energy. There are also two shoulders at 390 nm and 500 nm, which are tentatively, attributed to a metal to ligand charge transfer transitions involving 2,2′-bipyridine, 1,10-phenanthroline and the third ligand.

The FAB-MS of the prepared complexes have shown the fragmentation in the following way. First fragment was the ion pair $\{Ru(L)_2(L_1)\}^{2+}Cl^-$, followed by cation $\{Ru(L)_2(L_1)\}^{2+}$; and others are $\{Ru(L)(L_1)\}^{2+}$; $\{Ru(L)_2\}^{2+}$; $\{Ru(L)\}^{2+}$ respectively. This type of fragmentation was also observed for $[Ru(phen)_2(phi)]Cl_2$ and $[Ru(bpy)_2(phi)]Cl_2$[28] (bpy=2,2′-bipyridine; phen=1,10-phenanthroline; phi=9,10-phenanthrenequinonediimine) Spectrum 1.

Thus, based on the elemental analysis and spectral data, the proposed structures for the complexes are shown in Fig. 2.

Biological Activity and Discussion Results are summarized in Tables 1—3 and the pharmacological data were analyzed statistically by analysis of variance followed by Dunnett's test of significance. The statistical significance were considered only when $p<0.05$. All the complexes were tested for their anticancer activity against EAC bearing mice. Ru1—Ru4, Ru10 and Ru11 were found to increase the life span of the tumor hosts by 66—43% and were the most active in the series of synthesized complexes. Ru1—Ru4 was also found to bring the altered hemoglobin and RBC values of the EAC bearing mice to near normal values. The results of the present study clearly demonstrated the tumor inhibitory activity of the ruthenium complexes against transplantable murine tumor cell line (Table 1). In the EAC bearing mice, cells are present in the peritoneal cavity and the compounds were administered directly into the peritoneum. Thus, tumor inhibition might be due to the direct effect of the compounds on the tumor cells. The effect of these compounds on DNA synthesis is yet unknown but certain structurally-related tris-chelates of ruthenium are reported to have DNA binding property *in vitro*.[13] Studies on DNA binding of the synthesized complexes were performed and are reported in Table 4. Ru1—Ru4 show some interaction with calf thymus DNA as observed from their shift in the visible MLCT (metal to ligand charge transfer) bands.[29] Thus the action of these synthesized complexes could also be mediated *via* its

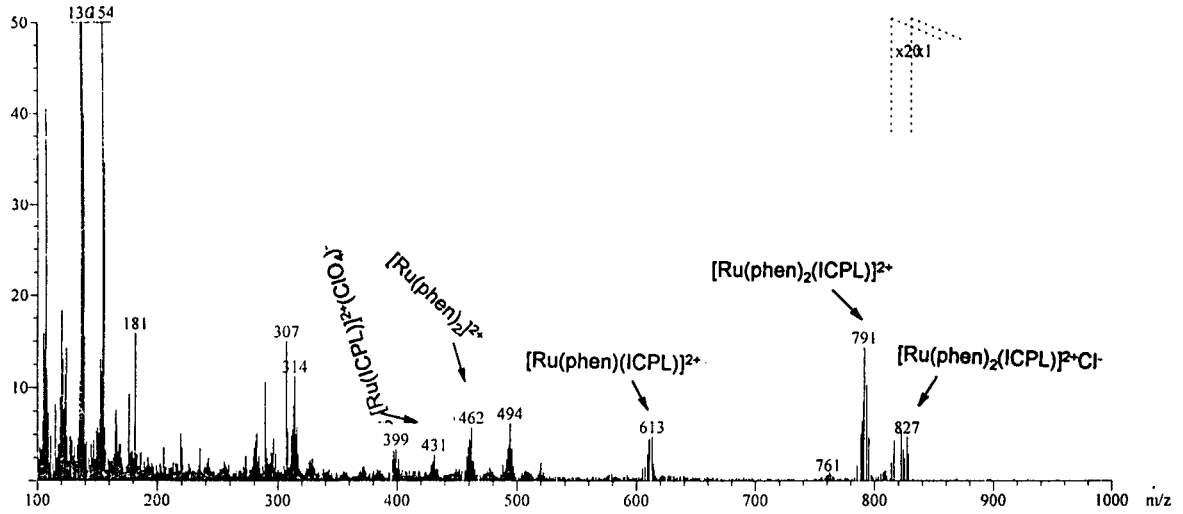

FAB-MS of the Ru3 complex in mNBA matrix

Spectrum 1

Table 1. Antineoplastic Activity of Ruthenium Complexes against EAC Bearing Mice

Treatment	Total body weight (g)	Mean survival time (d)	ILS (%)	Tumor volume (ml)	Viable cells in ascitic fluid (%)
Vehicle (5 ml/kg)	22.2±0.5	—	—	—	—
EAC (2×10^6 cells/mouse)	28.3±0.6	21	—	3.4±0.3	95.2±3.5
Cisplatin+EAC (2 mg/kg)	18.2±0.7	22	5	—	—
Ru1+EAC (2 mg/kg)	23.1±1.1	35	66	0.7±0.01	42.3±1.3
Ru2+EAC (2 mg/kg)	22.9±0.8	34	62	0.9±0.03	45.5±1.3
Ru3+EAC (2 mg/kg)	23.5±0.4	33	57	0.6±0.01	48.7±2.1
Ru4+EAC (2 mg/kg)	23.2±0.5	34	62	0.9±0.03	47.2±2.5
Ru5+EAC (2 mg/kg)	25.1±0.6	27	29	1.7±0.04	69.1±2.6
Ru6+EAC (2 mg/kg)	25.3±0.6	26	24	1.5±0.02	72.1±1.9
Ru7+EAC (2 mg/kg)	24.8±0.7	26	24	1.3±0.06	66.8±2.1
Ru8+EAC (2 mg/kg)	24.2±0.2	26	24	1.3±0.02	66.5±1.9
Ru9+EAC (2 mg/kg)	24.6±0.3	25	19	1.5±0.03	69.5±1.6
Ru10+EAC (2 mg/kg)	23.9±0.4	30	43	1.1±0.02	53.4±1.4
Ru11+EAC (2 mg/kg)	24.1±0.3	30	43	1.2±0.05	52.7±1.7
Ru12+EAC (2 mg/kg)	24.3±0.6	28	33	1.4±0.04	62.7±1.3

Values are mean±S.E.M.

Table 2. Effect of Ruthenium Complexes on the Hematological Profile of EAC Bearing Mice

Treatment	Hb (g/dl)	RBC (count$\times10^8$)	WBC (count$\times10^8$)	Lymphocyte (%)	Granulocyte (%)	Monocyte (%)
Vehicle (5 ml/kg)	12.2±0.3	12.1±1.1	6.7±1.1	71.3±2.4	2.1±0.2	26.6±0.4
EAC (2×10^6 cells/mouse)	9.3±0.6	6.52±0.8	17.2±2.9	62.5±2.7	33.3±0.8	4.2±1.2
Cisplatin+EAC (2 mg/kg)	10.1±0.4	5.6±0.3	10.1±1.8	65.3±3.1	29.3±2.1	5.4±0.3
Ru1+EAC (2 mg/kg)	11.8±0.4	6.2±0.5	9.5±0.8	77.8±4.1	4.7±0.3	17.5±0.8
Ru2+EAC (2 mg/kg)	11.5±0.2	6.3±0.5	9.3±0.6	77.4±2.8	4.8±0.4	17.8±0.3
Ru3+EAC (2 mg/kg)	11.1±0.3	6.2±0.2	9.7±0.5	77.3±2.1	5.2±0.7	17.5±0.7
Ru4+EAC (2 mg/kg)	11.4±0.4	6.0±0.4	9.6±0.4	77.7±2.2	4.8±0.6	17.5±0.4
Ru5+EAC (2 mg/kg)	9.3±0.1	5.2±0.3	11.5±1.1	80.9±3.1	8.9±0.9	11.2±0.5
Ru6+EAC (2 mg/kg)	9.1±0.3	5.1±0.2	10.2±1.2	81.5±1.4	8.5±0.2	11.0±0.6
Ru7+EAC (2 mg/kg)	9.8±0.4	5.7±0.6	10.8±0.8	79.1±1.1	7.1±0.1	13.8±0.5
Ru8+EAC (2 mg/kg)	9.7±0.3	5.5±0.8	10.3±0.6	78.6±2.1	7.3±0.4	14.1±0.8
Ru9+EAC (2 mg/kg)	9.3±0.5	5.3±0.2	11.7±0.4	80.2±2.4	7.3±0.2	12.5±0.4
Ru10+EAC (2 mg/kg)	10.2±0.4	5.9±0.7	8.9±0.6	79.7±2.1	5.2±0.3	15.1±0.6
Ru11+EAC (2 mg/kg)	10.1±0.5	5.9±0.6	8.8±0.3	79.8±3.1	5.4±0.6	14.8±0.6
Ru12+EAC (2 mg/kg)	9.8±0.3	5.8±0.7	10.1±0.5	83.1±1.9	6.2±0.4	10.7±0.6

Values are mean±S.E.M.

Table 3. Antibacterial Activity of Ruthenium Complexes at 200 μg/ml

Treatment	*Vibrio cholerae* 865	*Vibrio cholerae* 14033	*Staphylococcus aureus* 6571	*Staphylococcus aureus* 8530	*Shigella flexnari*	*Shigella sonnei*
Ru1	16±0.2	10±0.1	12±0.2	11±0.1	12±0.2	10±0.2
Ru2	15±0.1	10±0.2	11±0.2	12±0.2	13±0.2	10±0.1
Ru3	13±0.2	12±0.1	10±0.1	8±0.2	11±0.3	10±0.1
Ru4	12±0.2	8±0.2	9±0.2	9±0.2	10±0.3	9±0.2
Ru5	9±0.3	8±0.2	11±0.2	8±0.3	9±0.1	8±0.2
Ru6	11±0.2	9±0.1	10±0.1	12±0.2	8±0.1	10±0.1
Ru7	17±0.2	12±0.2	20±0.1	15±0.1	16±0.1	15±0.3
Ru8	20±0.1	14±0.2	20±0.1	12±0.1	19±0.2	16±0.3
Ru9	20±0.2	10±0.1	17±0.2	16±0.1	15±0.2	13±0.1
Ru10	16±0.2	11±0.1	18±0.1	15±0.3	16±0.1	13±0.2
Ru11	15±0.1	11±0.2	18±0.1	15±0.2	16±0.3	13±0.2
Ru12	14±0.1	10±0.2	17±0.1	16±0.2	15±0.1	12±0.1
STD	30±0.2	20±0.2	26±0.2	26±0.3	20±0.2	19±0.2

Values are mean±S.E.M. STD=Chloramphenicol 10 μg/ml. Zone of inhibition in mm (including bore size of 6 mm).

Table 4. Effects of Binding to DNA on Visible MLCT Transitions

Complexes	λ_{max} (nm)		$\Delta\lambda$ (nm)
	without DNA	with DNA	
Ru1	550	557	7
Ru2	555	561	6
Ru3	550	558	8
Ru4	545	555	10
Ru5	470	470	0
Ru6	465	465	0
Ru7	480	480	0
Ru8	460	460	0
Ru9	475	475	0
Ru10	470	470	0
Ru11	475	475	0
Ru12	480	480	0

Table 5. Physical Data for R-TSC (TSC=Thiosemicarbazide)

R	Melting point (°C)	Yield (%)
CH_3	135.5 (137)	48
C_2H_5	81—82 (84)	60
Cyclohexyl	142.5 (143)	53
4-Cl-phenyl	178 (180)	65
4-Br-phenyl	163—165	55
4-C_2H_5O-phenyl	175—177	68

Parentheses indicate literature melting point.

effect, if any, on the DNA.

Myelosupression is a frequent and major complication of cancer chemotherapy. Compared to the EAC control animals, ruthenium treatment and subsequent tumor inhibition resulted in appreciable improvements in hemoglobin content, RBC and WBC counts (Table 2). These observations assume great significance as anemia is a common complication in cancer and the situation aggravates further during chemotherapy since a majority of antineoplastic agents exert suppressive effects on erythropoiesis[30,31] and thereby limiting the use of these drugs. Cisplatin is known to cause bone marrow depression and acute nephrotoxicity. Thus, the severe depression of the bone marrow coupled with acute nephrotoxicity[32—35] probably caused a negative nitrogen balance in the cisplatin treated animals, which resulted in a loss of body weight. The nephrotoxicity of cisplatin is due to the capability of the compound to generate free radicals and reactive oxygen species within the liver and kidney.[36—43] The improvement in hematological profile of the tumor bearing mice following the treatment with ruthenium complexes could be secondary to tumor regression or due to the action of the compounds itself.

The complexes were also evaluated for its antibacterial activity by cup-plate method.[44] Significant antibacterial activity was observed for Ru7, Ru8 and Ru9 against the microorganisms *Vibrio cholerae* 865, *Staphylococcus aureus* 6571, *Shigella flexnari* and *Shigella sonnei* as compared to that of the standard drug chloramphenicol. Moderate activities were observed for Ru1—Ru4 and Ru10—Ru12 against the microorganisms *Vibrio cholerae* 865, *Staphylococcus aureus* 6571 and *Shigella flexnari*. However, all the complexes failed to show significant antibacterial activity against *Vibrio cholerae* 14033 and *Staphylococcus aureus* 8560. The enhanced antibacterial activity was observed for complexes with alkyl substituted thiosemicarbazides and $Ru(phen)_2Cl_2$. This increase in activity may be associated with larger ring size of phenanthroline moiety and the presence of alkyl substituents which together make the complexes more lipophillic.[18]

In the present study it can be clearly seen that the substitution of the central metal atom of the complexes with different ligands provides a major source of variation among the observed biological activities. Complexes bearing the ligands such as nmit and icpl were found to be more biologically active than complexes with aze. Thus it seems that the size as well as the substituent groups in the ligands influence biological activities of the complex. Further the presence of 1,10-phenanthroline imparted greater biological activity to the complexes than their 2,2′-bipyridine containing counterparts. Other workers in various studies involving *in vitro* models have also noted this fact.[29]

Conclusions

The results of the present study are encouraging as these compounds exhibit significant reduction in the tumor burden and caused prolongation of lifespan of the tumor hosts. Improvements, rather than aggravation, or tumor associated hematological complications such as anemia and bone mar-

row suppression were also noticed.

Experimental

Melting points were determined on an open capillary method and were uncorrected. Infra red (IR) spectra were recorded on a Jasco V 410/Shimadzu IR spectrometer. ^{1}H-NMR spectra were recorded on a Bruker Ultraspec (500/300 MHz) and the chemical shifts are given in δ values. The reported chemical shifts were against TMS. UV/visible spectra were run on Beckmann DU 64 UV spectrophotometer. FAB Mass spectra were recorded on a JEOL JMS 600 mass spectrometer in mNBA matrix. Elemental analysis for carbon, hydrogen and nitrogen were performed on a Perkin-Elmer 2400 elemental analyzer. Silica gel (SRL Mumbai). Acetazolamide (Leaderle, Mumbai), Sodium perchlorate (Fluka, U.S.A.).

Preparation of Isatin In a round-bottomed flask 9 g (0.05 mol) of chloral hydrate in 85 ml of water was placed. To this mixture 7 g of sodium sulfate and a solution of 3.1 g (0.03 mol) aniline in 20 ml of H_2O containing 4.1 g concentrated H_2SO_4 (sp.gr., 1.84) was added to dissolve the amine and finally a solution of 7 g (0.1 mol) of hydroxylamine hydrochloride in 17 ml of H_2O were added in the flask. It was then added at a rate such that vigorous boiling begins in about 40—45 min. After 1—2 min of vigorous boiling the reaction was complete. During the heating period some of the isonitroso acetanilide separated out. On cooling the solution in running water the remainder was crystallized. It was filtered with suction, dried in air. Yield 76%.

Twenty grams of concentrated H_2SO_4 (sp.gr., 1.84) was heated to 50 °C and then 5.4 g (0.03 mol) of dry isonitroso acetanilide was added in such a rate as to keep the temperature between 60—70 °C external cooling was applied at this stage so that the reaction could be carried out more rapidly. After the addition of all isonitroso acetanilide, the solution was heated to 80 °C and was kept at this temperature for about 10 min to complete the reaction. Then the reaction mixture was cooled to room temperature and poured upon ten to twelve times its volume of crushed ice. After standing for about 90 min the product was filtered with suction and washed with cold H_2O to remove the H_2SO_4. The crude product was then dried in air.

Purification of Isatin Two grams of crude isatin was suspended in 10 ml of hot water and treated with a solution of 0.5 g of NaOH in 2 ml of water. The solution was stirred and the isatin passes into solution. Dilute HCl was then added with stirring until a slight precipitate appears. The mixture was then filtered at once and the precipitate is rejected. The filtrate was made acid to Congo red paper and isatin slowly crystallizes out. It was filtered with suction and dried. mp 178 °C (lit.[45] 180 °C), yield 68%.

Preparation of N–CH_3–Isatin To a suspension of isatin (2 g) in ethanol (30 ml), ethanolic KOH (10 ml, 10%) added portionwise during 20 min, with shaking. To the deep purple suspension, dimethyl sulfate (freshly distilled, 1.5 ml) was added and the reaction mixture was shaken for 30 min. The mixture was filtered and ethanol (25 ml) removed from the filtrate by distillation. The residue from the filtration was added to hot water (6 ml), the concentrated alcoholic solution was added and the mixture heated to give a clear solution. On cooling, *N*-methylisatin (1.50 g, 60%) separated as orange needles. mp 134 °C (lit.[46] 136 °C).

Preparation of NMIT In a round bottom flask fitted with a reflux condenser *N*-methylisatin 0.16 g (1 mmol), thiosemicarbazide (TSC) 0.09 g (1 mmol) and glacial acetic acid (0.5 ml) were added. The mixture was refluxed in alcohol for 3 h and left overnight. It was filtered through Buchner flask and purified by column chromatography over silica gel (60—120 mesh) by using $CHCl_3$–EtOAc (7 : 3) as the eluate.

NMIT: Yield 60%, yellow fiber, mp 226—228 °C (decomposition). IR (KBr) cm^{-1}: 3425—3151 (NH_2 and NH), 1678 (C=O), 1608 (N–H def) and 1372—1340 (C=S). *Anal.* Calcd for $C_{10}H_{10}N_4OS$: C, 51.27; H, 4.30; N, 23.91. Found: C, 49.98; H, 4.19; N, 23.98.

Preparation of ICPL In a round bottom flask fitted with a reflux condenser isatin 0.14 g (1 mmol), 4-chloro-phenyl-thiosemicarbazide (PTSC) 0.20 g (1 mmol) and glacial acetic acid (0.5 ml) were added. The mixture was refluxed in alcohol for 15 h and left overnight. It was filtered through Buchner flask and purified by column chromatography over silica gel (60—120 mesh) by using $CHCl_3$–EtOAc (7 : 3) as eluate.

ICPL: Yield 55%, yellow fibre, mp 238—240 °C (decomposition). IR (KBr) cm^{-1}: 1693 (C=O), 1621 (N–H def) and 1397—1346 (C=S). *Anal.* Calcd for $C_{15}H_{11}ClN_4OS$: C, 54.46; H, 3.35; N, 16.94. Found: C, 54.27; H, 3.50; N, 17.05.

Preparation of R-TSC One tenth mole of amine was dissolved in 20 ml of ammonium hydroxide (sp.gr. 0.88) and 8 ml of carbon disulfide was slowly added while stirring the mixture on ice. Until all the addition of carbon disulfide the temperature was kept below 15 °C, stirring was continued for further 30 min, then ethanol was added until all the carbon disulfide went into solution. The mixture was left to warm to room temperature for 2 h. During this time a white precipitate of the intermediate ammonium dithiocarbamate begins to form. Ten milliliters of 50% hydrazine hydrate and sodium chloroacetate (0.1 mol) is rapidly added in succession while the mixture is heated on a water bath. The clear solution formed is immediately filtered and the solution is reduced to half its original volume. The mixture is kept overnight at room temperature and the thiosemicarbazide formed crystallizes out (Table 4).

Preparation of *cis*-Bis(L)dichlororuthenium(II).[47] *cis*-[Ru(L)$_2$Cl$_2$] Where L=2,2′-bipyridine/1,10-phenanthroline $RuCl_3 \cdot 3H_2O$, 1.15 g (2.5 mmol) and L (5 mmol) was refluxed in 50 ml DMF for 3 h under nitrogen atmosphere. The reddish brown solution slowly turned purple and the product precipitated in the reaction mixture. The solution was cooled overnight at 0 °C. A fine microcrystalline mass was filtered off. The residue was repeatedly washed with 30% LiCl solution and finally recrystallised from the same. The product was dried and stored in a vacuum desiccator over P_2O_5 for further use (yield 75%).

Synthesis of Ru1 To the black microcrystalline *cis*-[Ru(phen)$_2$Cl$_2$] 1.064 g (2 mmol) ligand nmit 0.58 g (2.5 mmol) was added and refluxed in ethanol under nitrogen respectively. The reaction was monitored by TLC and the complexes were separated by column chromatography on silica support (230—400 mesh silica) using chloroform and methanol as eluate in an ascending order of polarity. After collecting the product, excess of solvent was distilled off and the resultant solution was kept at 0 °C overnight. A microcrystalline precipitate was obtained. The crystals were filtered and were dried over $CaCl_2$ in vacuum.

Yield 45%, black crystals, IR (KBr) cm^{-1}: 3251—3162 (N–H), 1690 (C=O), 1603 (N–H def), 1324 (C=S). UV/Vis λ_{max} (methanol) nm: 260, 400, 460, 550. ^{1}H-NMR (DMSO-d_6) δ: 9.65 (1H, d, J=5.15 Hz), 9.25 (1H, d, J=4.86 Hz), 8.82 (1H, d, J=7.76 Hz), 8.74 (1H, d, J=7.92 Hz), 8.51 (2H, d, J=8.32 Hz), 8.41 (1H, d, J=3.16 Hz), 8.39 (1H, d, J=4.07 Hz), 8.25 (1H, d, J=8.88 Hz), 8.19 (1H, d, J=5.20 Hz) 8.17 (1H, d, J=4.38 Hz), 8.12 (1H, d, J=8.86 Hz), 8.08 (1H, dd, J=8.16, 5.33 Hz), 8.00 (2H, s), 7.89 (1H, d, J=5.19 Hz), 7.62 (1H, d, J=4.77 Hz), 7.47 (1H, dd, J=8.09, 5.33 Hz), 7.41 (1H, dd, J=8.06, 5.36 Hz), 7.16 (1H, t, J=14.51 Hz), 6.87 (1H, t, J=15.15 Hz), 6.70 (1H, d, J=7.73 Hz), 5.31 (1H, s), 2.66 (3H, s). FAB-MS (mNBA): 731, $[Ru(phen)_2(nmit)]^{2+}Cl^-$; 695, $[Ru(phen)_2(nmit)]^{2+}$; 515, $[Ru(phen)(nmit)]^{2+}$; 460, $[Ru(phen)_2]^{2+}$; 335, $[Ru(nmit)]^{2+}$. *Anal.* Calcd for $C_{34}H_{26}Cl_2N_8ORuS$: C, 53.26; H, 3.39; N, 14.62. Found: C, 53.30; H, 3.25; N, 15.05.

Synthesis of Ru2 A similar synthetic procedure was adopted as for Ru1 with nmit as the third ligand except for the starting material which was *cis*-[Ru(bpy)$_2$Cl$_2$].

Yield 47%, black crystals, IR (KBr) cm^{-1}: 3258—3169 (N–H), 1697 (C=O), 1600 (N–H def), 1340 (C=S). UV/Vis λ_{max} (methanol) nm: 260, 405, 458, 555. FAB-MS (mNBA): 683, $[Ru(bpy)_2(nmit)]^{2+}Cl^-$; 647, $[Ru(bpy)_2(nmit)]^{2+}$; 492, $[Ru(bpy)(nmit)]^{2+}$; 413, $[Ru(bpy)_2]^{2+}$; 335, $[Ru(nmit)]^{2+}$. *Anal.* Calcd for $C_{30}H_{26}Cl_2N_8ORuS$: C, 50.14; H, 3.62; N, 15.60. Found: C, 49.98; H, 3.45; N, 16.03.

Synthesis of Ru3 With *cis*-[Ru(phen)$_2$Cl$_2$] as the starting material and icpl as the third ligand Ru3 was synthesized in a similar manner as Ru1.

Yield 48%, black crystals, IR (KBr) cm^{-1}: 3414 (N–H broad), 1699 (C=O), 1611 (N–H), 1321 (C=S). UV/Vis λ_{max} (methanol) nm: 258, 400, 455, 550. ^{1}H-NMR (DMSO-d_6) δ: 10.44 (1H, s), 10.02 (1H, s), 9.60 (1H, d, J=4.17 Hz), 9.24 (1H, d, J=4.17 Hz), 8.83 (1H, d, J=8.14 Hz), 8.75 (1H, d, J=8.18 Hz), 8.53 (1H, d, J=8.23 Hz), 8.44 (2H, m), 8.26—8.11 (6H, m), 8.09 (1H, dd, J=8.24, 5.37 Hz), 7.87 (1H, d, J=6.41 Hz), 7.65—7.62 (3H, m), 7.48 (1H, dd, J=8.19, 5.32 Hz), 7.40—7.35 (4H, m), 7.06 (1H, m), 6.66 (1H, m), 6.50 (1H, d, J=7.74 Hz). FAB-MS (mNBA): 827, $[Ru(phen)_2(icpl)]^{2+}Cl^-$; 809, $[Ru(phen)_2(icpl)]^{2+}H_2O$; 791, $[Ru(phen)_2(icpl)]^{2+}$; 613, $[Ru(phen)(icpl)]^{2+}$; 462, $[Ru(phen)_2]^{2+}$; 431, $[Ru(icpl)]^{2+}$. *Anal.* Calcd for $C_{39}H_{27}Cl_3N_8ORuS$: C, 54.29; H, 3.13; N, 12.99. Found: C, 54.25; H, 3.10; N, 13.15.

Synthesis of Ru4 With *cis*-[Ru(bpy)$_2$Cl$_2$] as the starting material and icpl as the third ligand Ru3 was synthesized in a similar manner as Ru1.

Yield 45%, black crystals, IR (KBr) cm^{-1}: 3400 (N–H broad), 1695 (C=O), 1625 (N–H), 1330 (C=S). UV/Vis λ_{max} (methanol) nm: 260, 405, 450, 545. FAB-MS (mNBA): 779, $[Ru(bpy)_2(icpl)]^{2+}Cl^-$; 743, $[Ru(bpy)_2(icpl)]^{2+}$; 587, $[Ru(bpy)(icpl)]^{2+}$; 413, $[Ru(bpy)_2]^{2+}$; 431, $[Ru(icpl)]^{2+}$. *Anal.* Calcd for $C_{35}H_{27}Cl_3N_8ORuS$: C, 51.59; H, 3.31; N, 13.76. Found: C, 51.25; H, 3.38; N, 14.05.

Synthesis of Ru5 To the black microcrystalline *cis*-Ru(phen)$_2$Cl$_2$ (2 mmol) ligand aze 0.55 g (2.5 mmol) was added and refluxed in ethanol

under nitrogen atmosphere. The reaction was monitored by TLC on silica gel plates. After the completion of reaction, the reaction mixture was cooled to room temperature. The complex was purified by column chromatography on neutral alumina using dichloromethane : isopropanol (19 : 1) as elutant. After collecting the product, excess of solvent was distilled off and the resultant solution was kept at 0 °C overnight. A microcrystalline precipitate was obtained. The crystals were filtered and were dried over $CaCl_2$ in vacuum.

Yield 47%: IR (KBr) cm^{-1}: 3401 (SO_2NH_2 and N–H), 3100 (C–H), 1641 (C=O), 1552—1428 (C=N), 1337—1288 (SO_2). UV λ_{max} (methanol) nm: 245, 286, 470. ^{1}H-NMR (DMSO-d_6) δ: 9.97 (1H, d, J=4.73 Hz), 8.80 (2H, t, J=16.78 Hz), 8.48—8.45 (2H, m), 8.36 (3H, td, J=9.80, 3.59 Hz), 8.13 (1H, dd, J=8.16, 5.35 Hz), 7.88 (2H, t, J=9.55 Hz), 7.55 (2H, dd, J=7.97, 5.36 Hz), 1.82 (3H, s). FAB-MS (mNBA): 683, $[Ru(phen)_2(aze)]^{2+}$; 503, $[Ru(phen)(aze)]^{2+}$; 460, $[Ru(phen)_2]^{2+}$; 323, $[Ru(aze)]^{2+}$. *Anal.* Calcd for $C_{28}H_{22}Cl_2N_8O_3RuS$: C, 44.56; H, 2.92; N, 14.85. Found: C, 44.25; H, 2.73; N, 15.02.

Synthesis of Ru6 With *cis*-$[Ru(bpy)_2Cl_2]$ as the starting material and aze as the third ligand Ru6 was prepared in a similar manner to Ru5.

Yield 45%: IR (KBr) cm^{-1}: 3450 (SO_2NH_2 and N–H), 3100 (C–H), 1643 (C=O), 1555—1425 (C=N), 1340—1290 (SO_2). UV λ_{max} (methanol) nm: 240, 280, 465. ^{1}H-NMR (DMSO-d_6) δ: 9.53 (1H, d, J=5.25 Hz), 8.72 (2H, t, J=13.67 Hz), 8.63 (2H, d, J=7.20 Hz), 8.14 (2H, dd, J=13.94, 6.30 Hz), 7.92—7.88 (3H, m), 7.80 (1H, t, J=12.47 Hz), 7.71 (1H, t, J=12.38 Hz), 7.60 (2H, dd, J=8.76, 5.64 Hz), 7.33 (2H, dd, J=12.01, 4.80 Hz), 1.88 (3H, s). FAB-MS (mNBA): 635, $[Ru(bpy)_2(aze)]^{2+}$; 479, $[Ru(bpy)(aze)]^{2+}$; 413, $[Ru(bpy)_2]^{2+}$; 323, $[Ru(aze)]^{2+}$. *Anal.* Calcd for $C_{24}H_{22}Cl_2N_8O_3RuS$: C, 40.79; H, 3.12; N, 15.86. Found: C, 40.50; H, 3.15; N, 16.05.

Synthesis of Ru7—Ru12 To the black microcrystalline *cis*-$Ru(phen)_2Cl_2$ (2 mmol), R-TSC (R-TSC=*N*-alkyl/*N*-aryl substituted thiosemicarbazides, where R denotes the substituent on the N4 atom of the thiosemicarbazide) (2.5 mmol) was added and refluxed in ethanol under nitrogen atmosphere. The initial purple colored solution slowly changed to a brownish orange at the end of the reaction, the reaction was verified by TLC on silica gel plates. The reaction mixture was cooled to room temperature. The complex was purified by column chromatography on silica support (230—400 mesh, silica gel) using chloroform and methanol as eluents in an ascending order. The pure complexes were dissolved in a minimum volume of dry ethanol. Excess cold solution of $NaClO_4$ was added to the mixture and the resultant solution cooled at 0 °C overnight. A microcrystalline precipitate was obtained. The crystals were filtered and dried over $CaCl_2$ in vacuum.

Ru7: Where R=CH_3.

Yield 45%, a brown microcrystalline powder, IR (KBr) cm^{-1}: 3290—3090 (NH_2), 3125 (N–H), 2980—2890 (C–H), 1669 (N–H_2 def), 1535 (N–C=S), 1384 (C=S). UV λ_{max} (methanol) nm: 255, 300, 365, 480. *Anal.* Calcd for $C_{26}H_{23}Cl_2N_7O_8RuS$: C, 40.78; H, 5.14; N, 12.81. Found: C, 40.75; H, 4.98; N, 12.95.

Ru8: Where R=C_2H_5.

Yield 48%, a brown microcrystalline powder, IR (KBr) cm^{-1}: 3293—3068 (NH_2), 3155 (N–H), 2985—2884 (C–H), 1653 (N–H_2 def), 1541 (N–C=S), 1389 (C=S). UV λ_{max} (methanol) nm: 240, 275, 340, 460. *Anal.* Calcd for $C_{27}H_{25}Cl_2N_7O_8RuS$: C, 41.59; H, 3.21; N, 12.58. Found: C, 41.40; H, 3.15; N, 12.70.

Ru9: Where R=cyclohexyl.

Yield 50%, a brown microcrystalline powder, IR (KBr) cm^{-1}: 3245—3060 (NH_2), 3230 (N–H), 2932—2855 (C–H), 1650 (N–H_2 def) 1574 (N–C=S), 1340 (C=S). UV λmax (methanol) nm: 245, 285, 335, 475. ^{1}H-NMR (DMSO-d_6) δ: 9.83 (1H, d, J=5.16 Hz), 9.22 (1H, d, J=7.57 Hz), 8.84—8.53 (2H, m), 8.51—8.02 (12H, m), 7.96 (1H, d, J=5.32 Hz), 7.77 (1H, dd, J=11.88, 5.27 Hz), 7.56 (1H, dd, J=13.30, 7.85 Hz), 7.48 (1H, t, J=13.37 Hz), 1.65 (5H, m), 1.24 (6H, m). FAB-MS (mNBA): 680, $[Ru(phen)_2(cyclohexyl\text{-}tsc)]^{2+}ClO_4^-$. *Anal.* Calcd for $C_{31}H_{31}Cl_2N_7O_8RuS$: C, 44.65; H, 3.72; N, 11.76. Found: C, 44.29; H, 3.76; N, 11.91.

Ru10: Where R=4-Cl-phenyl.

Yield 50%, a brown microcrystalline powder, IR (KBr) cm^{-1}: 3210—3078 (NH_2), 2950 (C–H), 1596 (N–H_2 def), 1557 (N–C=S), 1316 (C=S). UV δ_{max} (methanol) nm: 235, 295, 355, 470. *Anal.* Calcd for $C_{31}H_{24}Cl_3N_7O_8RuS$: C, 43.21; H, 2.79; N, 11.38. Found: C, 39.95; H, 2.86; N, 11.50.

Ru11: Where R=4-Br-phenyl.

Yield 40%, a brown microcrystalline powder, IR (KBr) cm^{-1}: 3250—3070 (NH_2), 3107—2900 (C–H), 1599 (N–H_2 def), 1525 (N–C=S), 1420 (C=S). UV λ_{max} (methanol) nm: 240, 300, 355, 475. *Anal.* Calcd for $C_{31}H_{24}Cl_2BrN_7O_8RuS$: C, 41.06; H, 2.65; N, 10.82. Found: C, 39.85; H, 2.82; N, 10.75.

Ru12: Where R=4-C_2H_5O-phenyl.

Yield 55%, a brown microcrystalline powder, IR (KBr) cm^{-1}: 3280—3071 (NH_2), 2978—2873 (C–H), 1663 (N–H_2 def), 1528 (N–C=S), 1340 (C=S). UV λ_{max} (methanol) nm: 245, 300, 360, 480. *Anal.* Calcd for $C_{33}H_{29}Cl_2N_7O_9RuS$: C, 47.09; H, 3.44; N, 11.65. Found: C, 47.02; H, 3.25; N, 11.80.

Evaluation of Therapeutic Effect *in Vivo* Albino Swiss mice (18—20 g body weight) were maintained in identical laboratory conditions and given standard food pellets (Hindustan Lever Ltd, Bombay, India) and water *ad libitum*. LD_{50} values of the synthesized complexes were evaluated according to the literature procedure.[48] The animals were divided into 15 groups each containing 10 mice. Group I was vehicle control (5 ml/kg body weight i.p.) and group II was Ehrlich Ascites Carcinoma control (EAC; 2×10^6 EAC cells/mouse i.p.). Group III was treated with standard drug cisplatin (2 mg/kg body weight). All the complexes, Ru1—Ru12 were administered (i.p.) at a dose of 2 mg/kg body weight to animals in groups IV—XV respectively. All the complexes (Ru1—Ru12) and cisplatin were administered daily for 9 d starting 24 h after tumor transplantation. Five animals from each group were sacrificed 18 h after the last dose. The ascitic fluid volume, ascitic cell counts and hematological parameters were noted. Mean survival time (MST) for remaining 5 mice of each group was noted.

Tumour Volume and Viable Count Ascites volume was noted by taking it in a graduated centrifuge tube and packed cell volume determined by centrifuging at 1000 ***g*** for 5 min. Viablity of ascitic cells were checked by trypan blue (0.4% in normal saline) dye exclusion test and the count was taken in Neubauer counting chamber. The effect of the ruthenium compounds on tumor growth was monitored by recording the mortality daily and percentage increase in life span (% ILS) was calculated by the following formula:

$$\text{ILS (\%)} = [(\text{mean survival of treated group})/\text{mean survival of control group}) - 1] \times 100$$

Hematological Studies[49] Blood was collected from the tail vein, 24 h after the last dose. For the total count blood was drawn into RBC or WBC pipettes, diluted and counted in a hemocytometer. Hemoglobin concentration was determined by a hemoglobinometer. Differential count of leukocyutes was done on freshly drawn blood film using Leishman's stain.

Evaluation of Antibacterial Activity[43] A stock solution of ruthenium complexes were 200 μg/ml was made in sterile water containing 5% DMF under aseptic conditions and further dilutions were made with the same solvent in a similar manner. All the dilutions and stock solutions were sterilized by membrane filtration. Solid agar and liquid broth culture media No. 1 were used for all the test organisms and the pH was adjusted to 7.2. Antimicrobial activity of the ruthenium complexes against different strains of bacteria was determined by cup-plate method, and activity was expressed in terms of diameters of zone of inhibition. Inoculum was prepared by washing a fresh 5 ml medium slant of test organisms with 5 ml sterile water and further diluting the 1 ml washing to 10 ml. This suspension (0.15 ml) was added to 15 ml melted medium at a temperature 45—50 °C and plates were prepared. Holes of diameter 6 mm were dug into the agar plates with a sterile borer and filled with the drug. The plates were incubated for at 35 °C for 24 h. The results were compared with that of standard chloramphenicol.

Effects of Binding to DNA on Visible MLCT Transitions[29,50] All the experiments involving the interaction of the complexes with DNA were carried out using 5 mM Tris buffer at pH 7.4 with 50 mM NaCl. Keeping the concentration of the complexes constant (2.5 μM) and varying the concentration of DNA (20—50 μg/ml), the absorption titration was carried out. Changes in the MLCT band of the complexes were noted. The shifts in the MLCT bands at the highest concentration of DNA are reported.

Acknowledgement The authors are thankful to All India Council for Technical Education (AICTE), New Delhi, for providing the funds for carrying research. Mr. Subhas S. Karki also expresses his thanks to Dr. R. Mukherjee, Dr. A. K. Banerjee and Dr. V. S. Giri, Indian Institute of Chemical Biology, Kolkata, India for their valuable help in performing spectral studies.

References and Notes

1) Clarke M. J., Zhu F., Frasca D. R., *Chem. Rev.*, **99**, 2511—2534 (1999).
2) Kureshy R. I., Khan N. H., *Polyhedron*, **12**, 195—201 (1993) and references theirin.
3) Chakravarty J., Bhattacharya S., *Polyhedron*, **15**, 1047—1055 (1996).

4) Baitalik S., Adhikary B., *Polyhedron*, **16**, 4073—4080 (1997).
5) Keppler B. K., Henn M., Juhl U. M., Berger M. R., Niebi R., Wagner F. E., *Prog. Clin. Biochem. Med.*, **10**, 41—69 (1989).
6) Novakova O., Kasparkova J., Vrana O., Van Vliet P. M., Reedijk J., Brabee V., *Biochemistry*, **34**, 12369—12378 (1995).
7) Vilaplana R. A., Gonzalez-Vichez F., Gutierrez-Puebla E., Ruiz-Valero C., *Inorg. Chim. Acta*, **224**, 15—18 (1994).
8) Sava G., Bergamo A., Zorzet S., Gava B., Casarsa C., Cocchietto M., Furlani A., Scarcia V., Serli B., Iengo E., Alessio E., Mestroni G., *Eur. J. Cancer*, **38**, 427—435 (2002).
9) Keppler B. K., Wehe D., Endres H., Rupp W., *Inorg. Chem.*, **26**, 844—896 (1987).
10) Keppler B. K., Rupp W., Juhl U. M., Endres H., Nieu R., Balzer W. S., *Inorg. Chem.*, **26**, 4366—4370 (1987).
11) Sava G., Ganglirdi R., Bergamo A., Alessio E., Mestroni G., *Anticancer Res.*, **19**, 969—972 (1999).
12) Cetinkaya B., Ozdemir I., Binbasioglu B., Durmaz R., Gunal S., *Arzneim.-Forsch./Drug. Res.*, **49**, 538—540 (1999).
13) Tysoe S. A., Morgan R. J., Baker D., Strekas T. C., *J. Phys. Chem.*, **97**, 1707—1711 (1993).
14) Smith C. A., Sunderland Smith A. J., Keppler B. K., Katz F., Baker E. N., *J. Biol. Inorg. Chem.*, **1**, 424—431 (1996).
15) Messori L., Kratz F., Alessio E., *Met.-Based Drugs*, **3**, 1—9 (1996).
16) Frasca D., Ciampa J., Emerson J., Umans R. S., Clarke M. J., *Met.-Based Drugs*, **3**, 197—209 (1996).
17) Clairs S. A., Paul J. D., *Platinum Metals Rev.*, **45**, 62—69 (2001).
18) Mazumder U. K., Gupta M., Bera A., Bhattacharya S., Karki S., Manikandan L., Patra S., *Indian J. Chem.*, **42A**, 313—317 (2003).
19) Lieber E., Pillai C. N., Hites R. D., *Can. J. Chem.*, **35**, 832—842 (1957).
20) Sen A. B., Sengupta S. K., *J. Ind. Chem. Soc.*, **39**, 628—634 (1962).
21) Nardelli M., Gasparri G. F., Battislini G. G., Musatti A., *Chem. Commun.*, **1965**, 187—188 (1965).
22) Gasparri G. F., Mangia A., Musatti A., Nardelli M., *Acta Crystallogr. B*, **24**, 367—374 (1968).
23) Campbell M. J. M., *Coord. Chem. Rev.*, **15**, 179 (1975).
24) Chattopadhyay S. K., Ghosh S. A., *Inorg. Chim. Acta*, **131**, 15—20 (1987).
25) Lieber E., Rao C. N., Pillai C. N., Ramachandran J., Hites R. D., *Can. J. Chem.*, **36**, 801—809 (1958).
26) Qi-Xiong Z., Qian-Lin Z., Jin-Ganf L., Bao-Hui Y., Liang-Nian J., Lei W., *J. Inorg. Biochem.*, **78**, 293—298 (2000).
27) Anna C. G. H., Marjolein E. T., Brockhui S., Aldrick H. V., Karlijn Van der S., Jaap G. H., Reedijk J., *Eur. J. Inorg. Chem.*, **2002**, 369—376 (2002).
28) Pyle A. M., Rehmann J. P., Meshoyrer R., Kumar C. V., Turro J. N., Barton J. K., *J. Am. Chem. Soc.*, **111**, 3051—3058 (1989).
29) Morgan R. J., Chatterjee S., Baker D. A., Strekas T. C., *Inorg. Chem.*, **30**, 2687—2692 (1991).
30) Prasad S. B., Giri A., *Ind. J. Expt. Biol.*, **32**, 155—162 (1994).
31) Doll D. C., Weiss R. B., *Cancer Treat. Rev.*, **10**, 185—200 (1983).
32) Beguin Y., *Acta Clin. Belg.*, **51**, 36—52 (1996).
33) Pispirigos K., Catsoulakos P., Karakiulakis G., *Biochem. Mol. Biol. Int.*, **31**, 565—573 (1993).
34) Ormond P. M., Basinger M. A., Jones M. M., Hande K. R., *J. Pharmacol. Exp. Ther.*, **262**, 246—251 (1992).
35) Valentovic M. A., Scott L. A., Madan E., Yokel R. A., *Toxicology*, **70**, 151—162 (1991).
36) Scott L. A., Madan E., Valentovic M. A., *Fundam. Appl. Toxicol.*, **12**, 530—539 (1989).
37) Tappel A. L., *Fed. Proc.*, **32**, 1870—1874 (1973).
38) Sadzuka Y., Shoji T., Takino Y., *Toxicol. Lett.*, **62**, 293—300 (1992).
39) Jeong J. C., Hwang W. M., Yoon C. H., Kim Y. K., *Nephron.*, **88**, 241—296 (2001).
40) Hara M., Yoshida M., Nishijima H., Yokosuka M., Ligo M., Ohtani-Kaneko R., Shimada A., Hasegawa T., Akama Y., Hirata K., *J. Pineal. Res.*, **30**, 129—138 (2001).
41) Saad S. Y., Najjar T. A., Noredinn A. M., Al-Rikabi A. C., *Pharmacol. Res.*, **43**, 193—198 (2001).
42) Antunes L. M., Darin J. D., Bianchi N de L., *Pharmacol. Res.*, **43**, 145—150 (2001).
43) Sener G., Satiroglu H., Kabasakal L., Arbak S., Oner S., Ercan F., Keyer-Uysa M., *Fundam. Clin. Pharmacol.*, **14**, 553—560 (2000).
44) National Committee for Clinical Laboratory Standards (NCCLS). Performance standards for antimicrobial disk susceptibility tests, 6th ed.: Approved standard M2-A6. National Committee for Clinical Laboratory Standards, Wayne, PA, 1999.
45) Marvel C. S., Heirs G. S., "Organic Synthesis Collections," 2nd ed., Vol. I, ed. by Blatt A. H., John Wiley & Sons Inc., New York, 1941.
46) John H., Ingleby R. F., *J. Chem. Soc.*, **1958**, 3639—3640 (1958).
47) Giordano P. J., Bock C. R., Wrighton M. S., *J. Am. Chem. Soc.*, **100**, 6960—6966 (1978).
48) Litchfield J. T., Jr., Wilcoxon F., *J. Pharmacol. Exp. Ther.*, **96**, 99—113 (1958).
49) Dacie J. V., Lewis S. M., "Practical Hematology," J. A. Churchill Livingston, Medical Division of Longmann Gr., London, 1958, p. 38.
50) Vaidyanathan V. G., Nair B. U., *J. Inorg. Biochem.*, **91**, 405—412 (2002).